water

MDPI

Article

Changes in the Carbon and Water Fluxes of Subtropical Forest Ecosystems in South-Western China Related to Drought

Lei Zhou [1,2,*], Shaoqiang Wang [2,*], Yonggang Chi [1,2], Weimin Ju [3], Kun Huang [4], Robert A. Mickler [5], Miaomiao Wang [2] and Quanzhou Yu [6]

1 College of Geography and Environmental Sciences, Zhejiang Normal University, Jinhua 321004, China; chiyonggang@zjnu.cn
2 Key Lab of Ecosystem Network Observation and Modeling, Institute of Geographical Sciences and Natural Resource Research, Beijing 100101, China; wmmgis@126.com
3 International Institute for Earth System Science, Nanjing University, Nanjing 210093, China; juweimin@nju.edu.cn
4 Research Center for Global Change and Ecological Forecasting, School of Ecological and Environmental Science, East China Normal University, Shanghai 200062, China; huangkuncas@163.com
5 Department of Forestry and Environmental Resources, North Carolina State University, Raleigh, NC 27613, USA; ramickle@ncsu.edu
6 School of Environment and Planning, Liaocheng University, Liaocheng 252000, China; yuquanzhou2008@126.com
* Correspondence: zhoulei@zjnu.cn (L.Z.); sqwang@igsnrr.ac.cn (S.W.); Tel.: +86-138-1140-5158 (L.Z.); +86-10-64889666 (S.W.)

Received: 20 April 2018; Accepted: 20 June 2018; Published: 21 June 2018

Abstract: Drought impacts carbon and water fluxes of terrestrial ecosystems, which are strongly coupled. However, the magnitudes of response of carbon and water fluxes to drought are dependent on many processes, which are more complex than previously expected. Southern China experienced regional climatic perturbation events in the past decade and a two-year drought in 2009–2010. We used a terrestrial ecosystem model coupled with remotely sensed observations and metrological data to simulate the variations of net primary productivity (NPP), evapotranspiration (ET), and water-use efficiency (WUE) (i.e., NPP/ET) in south-western China during the period 2001–2010. Using the standard precipitation index (SPI) classifying different drought stresses, we also quantified the effect of drought on the ecosystem by comparing changes in modelled estimates of monthly WUE, NPP and ET under normal (i.e., baseline) and drought conditions (i.e., 2009 and 2010). The results indicated that NPP and ET showed synchronized declines in drought periods, with time-lag effects. Furthermore, drought-induced NPP decline was larger than ET reduction. An increasing trend in WUE from the moderate to extreme drought classes occurred not only in baseline conditions but also in drought conditions. Especially in the extreme drought period (January, 2010), WUE for the forest ecosystem typically showed a positive response to drought, indicating a drought-resilient forest ecosystem. Our study has important implications for understanding climate extreme effects on the carbon and water cycle of the forest ecosystem.

Keywords: climate extremes; drought; productivity; evapotranspiration; water-use efficiency; forest ecosystem; resilience

1. Introduction

Persistent droughts reduce vegetation greenness, biomass, productivity, and increase tree mortality [1–8]. The frequency, severity and incidence of droughts are expected to increase with

climate change [9–11]. Extreme climate events and their ecological impacts have been observed in the United States, Europe, Brazil and China [1,12–15]. The sustainability of terrestrial carbon and water cycles is strongly affected by the frequency and intensity of large-scale drought events, and all these disturbances have substantial impacts on ecosystem structure, species composition and function [16–18]. Hence, they are of great importance in exploring the impacts of droughts on the regional carbon budget and water resources and improving our ability to refine water management.

Water availability controls plant photosynthesis and influences plant growth, and thus affects net primary productivity (NPP), evapotranspiration (ET) and then water-use efficiency (WUE) [19,20]. The productivity of forest ecosystems is vulnerable to drought and temperature extremes [21] and many studies have reported a drought-induced reduction in NPP [1,3,22–24]. At the global scale, large-scale drought has reduced regional NPP from 2000 to 2009, especially in the Southern Hemisphere [3]. Regionally, the effect of drought on carbon dynamics has been focused in different regions such as Europe and the Amazon. In Europe, the drought and heatwave in 2003 substantially reduced vegetation productivity, leading to a large net carbon release into the atmosphere [1,22]. The 2005 and 2010 drought events had a total biomass carbon impact in Amazon forests [23,24]. ET, the sum of water lost to the atmosphere from the soil surface through evaporation and from canopy via plant transpiration, is a central process of the hydrological, energy and carbon cycles [25–28]. Given a similarity in responses of ET and photosynthesis to stomatal closure, ecosystem ET is also impacted by drought and has feedbacks upon productivity accelerating with climate change [18,27]. Evidence has shown that drought reduced both ecosystem NPP and ET simultaneously [27,29,30]. However, the magnitudes of NPP and ET responding to drought depend on forest types and environmental stress [31,32]. WUE, defined as the ratio of NPP to ET, measures the trade-off between the carbon gain and water loss of terrestrial ecosystems and highlights the linkage between biological processes (i.e., photosynthesis and transpiration) and physical process (i.e., evaporation). In general, drought suppresses both ecosystem productivity and ET simultaneously and, in turn, has a great impact on WUE [32]. Based on long-term flux data and the satellite product from MODIS, Ponce-Campos et al. (2013) found the responses of WUE to changes in water availability were different in drought and wet years, with WUE increasing in drought years across all biomes [33]. A model study by Tian et al. (2010) suggested that the sensitivity of WUE to water availability depended on ecosystem types, which indicated that WUE response to an increase in precipitation is higher for forests [34]. A global study based on MODIS data also showed that increases of WUE were found in forests under drought impact [18]. Thus, evaluating shifts in WUE over drought stress and sensitivities of its component (i.e., NPP and ET) helps us better understand the potential impacts of climate change on ecosystem carbon budgets and water resources.

Drought frequency has been increasing in southern regions of China which have usually received ample precipitation in the last decade [6,35]. The 2009/2010 drought in south-western China was the most severe drought in the last five decades [36]. The spring drought occurring in south-western China reduced regional annual gross primary productivity and net primary productivity in 2010 by 65 and 46 Tg C yr^{-1}, respectively [37]. In this study, our objective was to utilize remote-sensing data, meteorology data and an ecological model to identify intermittent drought events that occurred from 2009 to 2010 in south-western China and quantify the drought impacts on NPP, ET and WUE in different drought class.

2. Materials and Methods

2.1. Study Area

The study area comprises 5 provinces (Yunnan, Sichuan, Guizhou provinces, Chongqing Municipality, and Guangxi Zhuang Autonomous Region) in south-western China, which cover 1.35×10^6 km^2 and account for 14% of the land territory of China (Figure 1). The climate of the study area is typical of subtropical monsoon, characterized by hot/rainy summers and cold/dry

winters. The mean annual precipitation and the annual average temperature of this region was 1343 mm and 14.8 °C from 1971 to 2000. The soils in south-western China are dominated by severely eroded red soils and yellow soils (oxisols). Subtropical coniferous forests, mixed coniferous and broad-leaved forests, subtropical evergreen broad-leaved forests, tropical rain forests, and monsoon forests are the major forest types in this region [38].

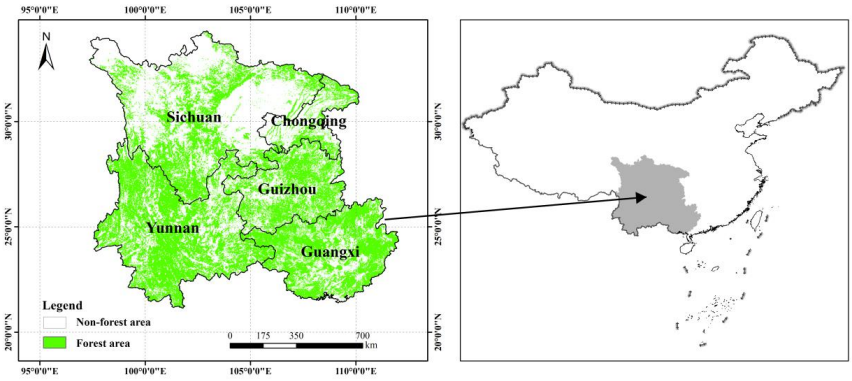

Figure 1. The location of south-western China's forests. Five provinces in south-western China experienced the 2009–2010 drought events.

2.2. Delineation of Drought Region

The standard precipitation index (SPI) for drought [39] was used to determine the drought events in the study area. SPI was calculated by fitting historical precipitation data to a Gamma probability distribution for the study time period and geographic area, and then transforming the Gamma function to a normal distribution [39]. The SPI has become an important tool for assessing moisture conditions based on monthly total precipitation. The remote sensing-based drought indices are mainly focused on using vegetation indices. Compared to remote-sensing data, meteorological data from weather stations generally cover longer periods of time and are more precise. As a result, SPI was selected in this study for its simplicity, temporal flexibility and spatial consistency. The 3-month SPI values were calculated using monthly precipitation data from 1972 to 2012. In our study, values of 3-month SPI between −0.99 and 0.99 denote average conditions (baseline conditions) and absolute values greater than 2.0 represent extreme conditions. The index classes (−1.99 to −1.50) and (−1.49 to −1.0) represent severe drought and moderate drought. On the basis of monthly 3-month SPI datasets, we calculated the mean SPI and minimum SPI during drought periods (Sep. 2009 to Mar. 2010) (Figure 2).

The soil moisture dataset from remote-sensing data was used as a proxy for soil water conditions in southern China. The global soil moisture dataset has been generated by active and passive microwave spaceborne instruments and covers the 32-year period from 1978 to 2010 (http://www.esa-soilmoisture-cci.org) at 0.25° resolution. The active data set was generated by the University of Vienna (TU Wien) based on obsesrvations from the C-band scatter meters on board the European Remote Sensing satellites (ERS-1/2) and Meteorological Operational satellite program (METOP-A). The passive data set was generated by the VU University Amsterdam in collaboration with the National Aeronautics and Space Administration (NASA) based on passive microwave observations from Nimbus 7 Scanning Multichannel Microwave Radiometer (SMMR), the Special Sensor Microwave Imager of the Defense Meteorological Satellite Program (DMSP SSM/I), the microwave imager from the Tropical Rainfall Measuring Mission microwave imager (TRMM TMI) and the Advanced Microwave Scanning Radiometer—Earth Observing System (AMSR-E) onboard the Aqua satellite. Due to a failure of the input sensors (ERS 2) in 2002–2005, the continuous soil moisture data from 2006 to 2010 was used in this study. The soil moisture dataset overlapped by the boundary of south-western China was used to detect changes in soil water condition of the forest ecosystem imposed by droughts during 2009–2010 in south-western China.

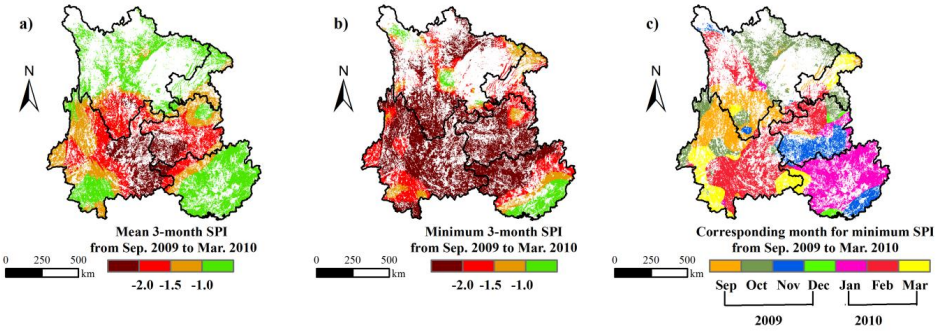

Figure 2. The area and extent of droughts in 2009 and 2010 based on 3-month standard precipitation index (SPI) from September 2009 to March 2010. (**a**) The mean 3-month SPI from September 2009 to March 2010; (**b**) minimum 3-month SPI from September 2009 to March 2010, which calculated by the minimum SPI during drought period based on pixel by pixel; (**c**) the corresponding month for minimum SPI during the drought period.

2.3. Ecosystem Measures of Net Primary Productivity (NPP), Evapotranspiration (ET) and Water-Use Efficiency (WUE)

The ecosystem functional indicators, i.e., NPP, ET, and WUE were used to explore the effects of carbon and the water cycle of the forest ecosystem in south-western China to 2009/2010 droughts events. Daily NPP, ET and WUE at a 1 km resolution for south-western China were derived from the national outputs of the BEPS (Boreal Ecosystem Productivity Simulator) model [40,41] and were summed to monthly scale from 2001 to 2010. These datasets were overlaid with a forest map of south-western China (Figure 1) at a 1 km resolution. We estimated monthly WUE using NPP (gC/m^2/month) and ET (mm/month), which links carbon and water cycles that is a key index of ecosystem function [42], and reflects "trade-off" relationship between carbon assimilation and water loss of terrestrial ecosystems [43]. Process models incorporate eco-physiological mechanisms to estimate carbon and water flux at daily time steps, and thus can be used to diagnose regional WUE.

2.3.1. Regional Scale Carbon and Water-Cycle Model

The BEPS model, which was developed from the FOREST-BGC model [44], was used to simulate carbon and water cycles of terrestrial ecosystems within the study area. The model includes a two-leaf (sunlit and shaded leaves) photosynthesis module that scales the leaf, using the Farquhar biochemical growth model [45], up to the canopy level with a new spatial and temporal scaling scheme [41]. Gross primary productivity (GPP) was calculated as the sum of sunlit and shaded GPP. NPP was calculated as the difference between GPP and autotrophic respiration (maintenance respiration and growth respiration). ET was calculated by separate sunlit and shaded leaves with the Penman–Monteith model [46]. The BEPS model has been improved to estimate the carbon and water fluxes of terrestrial ecosystems in many regions, for example, China [47–49], North America [50,51], East Asia [52], and at the global scale [53]. The model has been calibrated and validated using eddy covariance data in southern China [51] and has been used to demonstrate the ability of capturing the effect of disturbances [48].

2.3.2. Model Input Data

Meteorology data: Regional daily meteorology data (maximum air temperature, minimum air temperature, relative humidity, total precipitation, and sunshine duration) for the whole China at a resolution of 1 km × 1 km were obtained by using the ANUSPLIN algorithm to interpolate the 674 meteorology stations' data (provided by the Chinese National Meteorological Information Centre) to 1-km resolution pixels. Daily incoming solar radiation data was only observed in 122 stations, and missing data was generated by the Angstrom equation and inputs from the empirical relationship

between radiation and sunshine duration in the rest of the meteorological stations according to the method of Zhu et al., (2010) [54].

Remote-sensing data: In the BEPS model, land-cover information is used to specify plant physiological parameters that differ among land cover types. The land-cover map for the study area was derived from a nation-wide land-use map at a 30-m resolution that was interpreted from Landsat TM images and a 1:2,500,000 vegetation map [47]. The vegetation map was resampled with the same resolution as the land-use map, and the each forest pixel in the land-use map was assigned a forest type based on the vegetation map using the cell-to-cell function in ArcGIS [47]. The land-cover map has been validated with the site data and other satellite data (i.e., GLC2000) [47]. The 8-day leaf area index (LAI) dataset at a 1 km resolution from 2001 to 2010 were inverted using the MODIS reflectance product (MOD09A1 V05) and the 4-scale geometric optical model [49,55]. The locally adjusted cubic-spline capping (LACC) method [56] was used to smooth abrupt fluctuations of inversed 8-day LAI caused by residual cloud contamination [49]. In the BEPS model, we assumed the LAI was unchanged in the 8 day interval. The quality of retrieved LAI has been validated with the observation data in 6 regions in China [49]. The remote-sensing data that were of high quality can be used to drive the simulation of carbon and water cycle of forests in south-western China.

Soil data: The soil spatial database of physical soil properties for sand, silt, and clay fractions at a 1 km resolution was generated using the soil map and soil profiles from the Second National Soil Survey of China [57]. In this study, the soil texture datasets were used to determine hydrological parameters including the wilting point (water potential at 1500 kPa), field capacity (water potential at 33 kPa), porosity, saturated hydrological conductivity, air entry water potential and suction at saturation [49].

2.4. Study Design

Based on the monthly datasets (NPP, ET and WUE) from 2001 to 2010, we defined mean monthly baseline values for NPP, ET and WUE under normal conditions (i.e., monthly SPI values between –0.99 and 0.99). For each month during 2001–2008, all pixels under normal conditions defined by monthly SPI value between −0.99 and 0.99 were masked, which were used to extract monthly baseline values for NPP, ET and WUE (Equation (1)). Each monthly baseline layer in all years (2001–2008) was averaged to develop a mean monthly baseline layer (Equations (2)–(4)). On the basis of a drought class map (Figure 2b), we calculated the monthly baseline condition for NPP, ET and WUE by averaging over drought classes.

$$\mathrm{Flag}_j = \begin{cases} 0; \text{if } \mathrm{SPI}_j > 0.99 \text{ and } \mathrm{SPI}_j < -0.99 \ (j = 1, 2, 3 \ldots, n \times 12) \\ 1; \text{if } \mathrm{SPI}_j \leq 0.99 \text{ and } \mathrm{SPI}_j \geq -0.99 \ (j = 1, 2, 3 \ldots, n \times 12) \end{cases} \quad (1)$$

$$\mathrm{NPP\_baseline}_i = \frac{\sum_{k=1}^{n} \left(\mathrm{NPP}_{i+(k-1)\times 12} \times \mathrm{Flag}_{i+(k-1)\times 12} \right)}{\sum_{k=1}^{n} (k \times \mathrm{Flag}_{i+(k-1)\times 12})} \ (i = 1, 2, 3 \ldots 12) \quad (2)$$

$$\mathrm{ET\_baseline}_i = \frac{\sum_{k=1}^{n} \left(\mathrm{ET}_{i+(k-1)\times 12} \times \mathrm{Flag}_{i+(k-1)\times 12} \right)}{\sum_{k=1}^{n} (k \times \mathrm{Flag}_{i+(k-1)\times 12})} \ (i = 1, 2, 3 \ldots 12) \quad (3)$$

$$\mathrm{WUE\_baseline}_i = \frac{\sum_{k=1}^{n} \left(\mathrm{WUE}_{i+(k-1)\times 12} \times \mathrm{Flag}_{i+(k-1)\times 12} \right)}{\sum_{k=1}^{n} (k \times \mathrm{Flag}_{i+(k-1)\times 12})} \ (i = 1, 2, 3 \ldots 12) \quad (4)$$

where, n equal to 8, which denotes the non-drought years from 2001 to 2008; k is the year number from 1 to n; i is the month index. So Flag_i represented baseline condition (non-drought), and the $\mathrm{NPP\_baseline_i}$, $\mathrm{ET\_baseline_i}$ and $\mathrm{WUE\_baseline_i}$ denoted that average non-drought NPP, ET and WUE at time i, respectively. So, we defined the three variables: NPP_baseline, ET_baseline and WUE_baseline from January to December are the baseline seasonal variations of NPP, ET and WUE.

The monthly drought condition for NPP, ET and WUE was calculated from monthly ecosystem measures (NPP, ET and WUE) in the years 2009 and 2010. All monthly drought layers were summed to develop two annual drought layers (2009 and 2010) that can be compared with the normal conditions. Deviations from baseline conditions are denoted by Δ for all variables. We calculated the ecosystem measures under normal and drought conditions by averaging over drought class regions (i.e., three classes: moderate drought, severe drought and extreme drought). To remove the effects of possible changes in vegetation types, we classified the time series of mean monthly NPP, ET and WUE under normal conditions and drought conditions for each vegetation types, which were used to explore the drought impacts on carbon and water fluxes of south-western China's forests.

3. Results

3.1. The Model Validation with Eddy Covariance Flux Data

Monthly modelled GPP from the BEPS model was validated with eddy covariance (EC) flux data of forests in China. EC flux data were observed at three ChinaFLUX sites, Changbaishan temperate broad-leaved Korean pine mixed forest (CBS), Qianyanzhou subtropical coniferous plantation (QYZ) and Dinghushan subtropical evergreen broadleaved forest (DHS) [58]. The model performed well at the CBS and QYZ sites for GPP and ET (Figure 3a,b,d,e). The R^2 between modelled and observed GPP in three sites ranged from 0.47 to 0.97. The BEPS model also produced the seasonal pattern of ET well in three forest sites, which the R^2 values ranged from 0.75 to 0.90 (Figure 3). The R^2 between modelled and observed WUE was above the 0.001 significant levels at all 3 flux sites. The BEPS overestimated seasonal variations of WUE at the DHS site, while the variation of modelled WUE was a little higher than the measured values (Figure 3i). Furthermore, mean annual modelled WUE at CBS, QYZ and DHS during 2003–2010 were about 2.12 ± 0.13 gC/mm, 3.21 ± 0.22 gC/mm and 3.67 ± 0.21 gC/mm, respectively. The measurements from ChinaFLUX sites showed that mean annual WUE at CBS, QYZ and DHS during 2003–2008 were about 2.53 ± 0.23 gC/mm, 2.29 ± 0.33 gC/mm and 2.02 ± 0.16 gC/mm [59]. Our modelled data were consistent with previous literature [58,59].

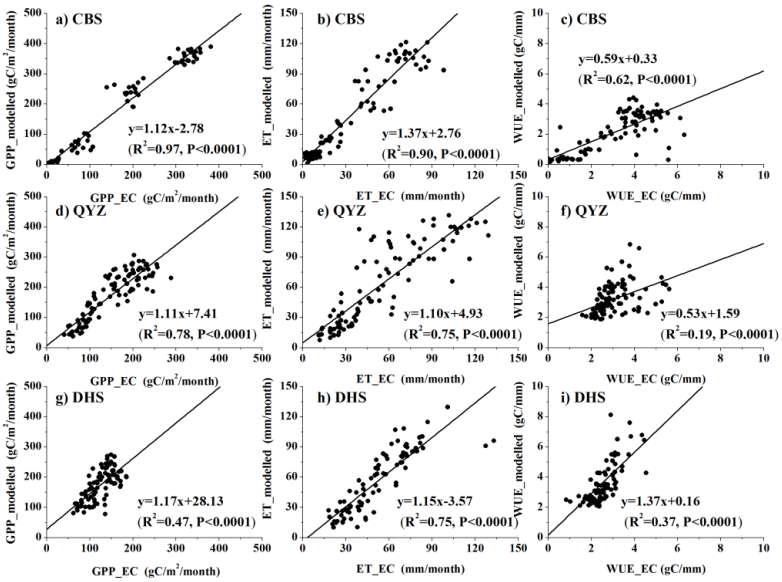

Figure 3. The validation of modeled monthly gross primary productivity (GPP), evapotranspiration (ET) and water-use efficiency (WUE) with eddy covariance flux data for three forest sites in China. CBS (**a**–**c**), Changbaishan temperate broad-leaved Korean pine mixed forest; QYZ (**d**–**f**), Qianyanzhou subtropical coniferous plantation: DHS (**g**–**i**), Dinghushan subtropical evergreen broad-leaved forest. All monthly data were from 2003–2010, except for DHS (2003–2009).

3.2. The Drought Characteristics of South-Western China in 2009 and 2010

Figure 2 shows the spatial distribution of the drought area and intensities indicated by average 3-month SPI from September 2009 to March 2010. We can see that the extreme drought event (SPI < −2.0) mainly occurred in Yunnan, Guizhou provinces and to a small extent in Guanxi province (Figure 2a). Furthermore, minimum SPI was derived by monthly SPI during September 2009 to March 2010 based on pixel by pixel analysis (Figure 2b). This indicated that almost 62% of south-western China expressed extreme drought during September 2009 to March 2010. But the time when the minimum monthly SPI occurred was different (Figure 2c). In the extreme drought area, the minimum SPI in nearly 30% and 22% region appeared in November 2009 and January 2010, respectively.

Here, we used soil moisture derived from spaceborne microwave during the drought period from September 2009 to March 2010 as a proxy for soil water content, showing that the absolute values of soil moisture in the surface layer of forest ecosystem in south-western China were indeed lower than mean value averaged over 2006–2008 (Figure 4), which was consistent with the SPI. The monthly soil moisture decreased by 18.5% (November 2009), 19.1% (December 2009), 18.8% (January 2010), 18.7% (February 2010) and 19.4% (March 2010) compared with the monthly mean of soil moisture from 2006 to 2008, respectively. This demonstrated that soil moisture was significantly reduced by the drought, which further confirmed the occurrence of extreme drought.

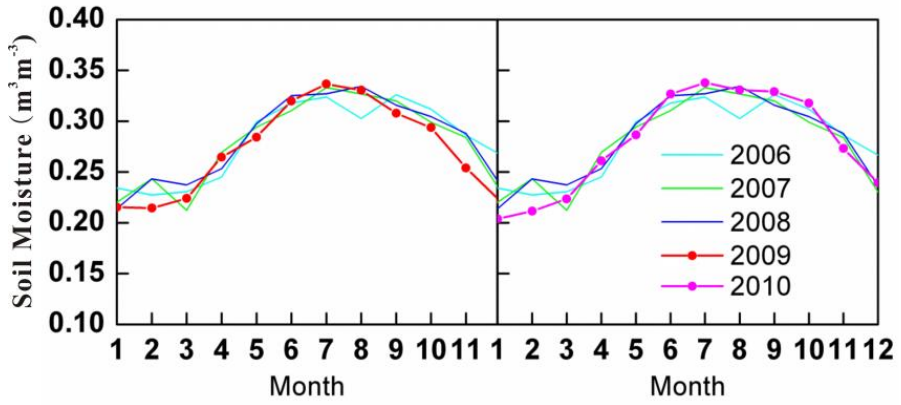

Figure 4. The inner-annual variation of soil moisture derived from microwave information during 2006–2010 in south-western China. The soil moisture in two drought years was separately compared to the baseline conditions (2006–2008).

3.3. Impacts of Drought on Forest Ecosystem Measures of NPP, ET and WUE

Mean annual baseline conditions and drought conditions of NPP, ET and WUE by three drought classes (D1: moderate drought, D2: severe drought and D3: extreme drought) was calculated in Table 1. The results indicated that the NPP and ET under normal conditions and drought conditions in severe drought regions were all larger than that in the other two drought classes. Thereby, WUE under baseline conditions and drought conditions were highest in the extreme drought region, followed by the severe drought region. Based on one-way Analysis of Variance (ANOVA), significant differences of NPP ($p < 0.0001$), ET ($p < 0.0001$) and WUE ($p < 0.0001$) can be found between drought classes (Table 1). The spatial distributions of baseline NPP, ET and WUE vs. NPP, ET and WUE under the drought condition (i.e., 2009 and 2010) were compared in Figure 5. Annual NPP in 2010 showed a pattern of lower than normal values in almost 61% of forest area in south-western China (Figure 5e). The highest reduction of NPP in a drought period (2009 and 2010) was found in the central part of Yunnan province, with an annual reduction of 100 gC/m^2 (Figure 5d,e). The highest increment of ET in a drought period (2009 and 2010) was mainly found in south-west and north-west parts of the study region (Figure 5i,j). The ratios of forest area in 2009 and 2010 that exhibited declines in ET under drought conditions are 73% and 59%, respectively. In 2009, just 30% of forest area showed an increasing

trend in WUE under drought conditions. However, the ratio of forest area in 2010 that exhibited an increment in WUE under drought conditions increased to 54%. In the D1 region (Moderate drought), NPP and ET in 2009 declined by 78 $gC/m^2/yr$. and 28 mm/yr related to baseline values. In the D2 region (severe drought), NPP and ET in 2009 declined by 75 $gC/m^2/yr$. and 14 mm/yr related to baseline values (Table 1, Figure 5). Furthermore, the reduction of NPP and ET in 2009 compared to baseline values was similar to that in the D1 region, with the values of 74 $gC/m^2/yr$ and 22 mm/yr. The annual WUE in 2009 in three drought classes was a little higher than in the baseline condition (Table 1, Figure 5). In 2010, the changes in NPP and ET in each drought class were not obvious (Table 1, Figure 5). The annual WUE in 2010 was a little higher than that in 2009 for each drought class.

Table 1. Mean annual net primary productivity (NPP) ($gC/m^2/yr$), ET (mm/yr) and WUE (gC/mm) under baseline conditions and drought conditions by three drought class. Drought class: D1: Moderate drought; D2: Severe drought; D3: Extreme drought.

Drought Class		D1	D2	D3
Baseline condition	**NPP**	762.8 ± 321.63c	854.7+391.94a	794.7 ± 370.0b
	ET	635.4 ± 171.9b	637.4 ± 160.1a	576.8 ± 146.6c
	WUE	1.19 ± 0.48c	1.31 ± 0.51b	1.35 ± 0.55a
Drought condition (2009)	**NPP**	684.6 ± 310.8c	780.1 ± 383.6a	721.2 ± 358.5b
	ET	607.1 ± 173.6b	623.8 ± 160.7a	555.1 ± 137.6c
	WUE	1.24 ± 0.56c	1.37 ± 0.62b	1.38 ± 0.67a
Drought condition (2010)	**NPP**	746.9 ± 320.3c	824.0 ± 380.6a	750.8 ± 352.4b
	ET	633.8 ± 176.9b	639.1 ± 162.3a	565.5 ± 142.1c
	WUE	1.30 ± 0.55c	1.41 ± 0.59b	1.42 ± 0.65a

Note. Values sharing the same letters in row are not different at $p < 0.05$ (by LSD test).

The time series of NPP, ET, and WUE under the normal condition and the drought condition were extracted by drought class (Figure 6). The seasonal pattern of NPP and ET showed a single peak for both baseline and drought conditions. The baseline NPP and NPP under drought conditions in the moderate drought region exhibited no differences in the second half of the drought period (Sep. 2009 to March 2010) (Figure 6a). Meanwhile, no differences could be found between ET under normal and drought conditions in the moderate drought region during the drought period (Figure 6d). In the severe drought region, NPP and ET under drought conditions during the drought period showed smaller values than that under normal conditions. The fact that drought directly reduced the NPP and ET during drought periods can also be found in the extreme drought region. The seasonal pattern of WUE under normal and drought conditions showed the lowest values in summer. In the first half of the drought period, WUE under the drought condition was obviously smaller than that under normal conditions in moderate and severe drought-class regions. But in the beginning of 2010, WUE under drought conditions exceeded the WUE values under normal conditions in these two drought-class regions. However, in the extreme drought region, WUE under drought conditions were close to the values under normal conditions in the first half of the drought period and then dramatically exceeded the baseline WUE in the second part of the drought period.

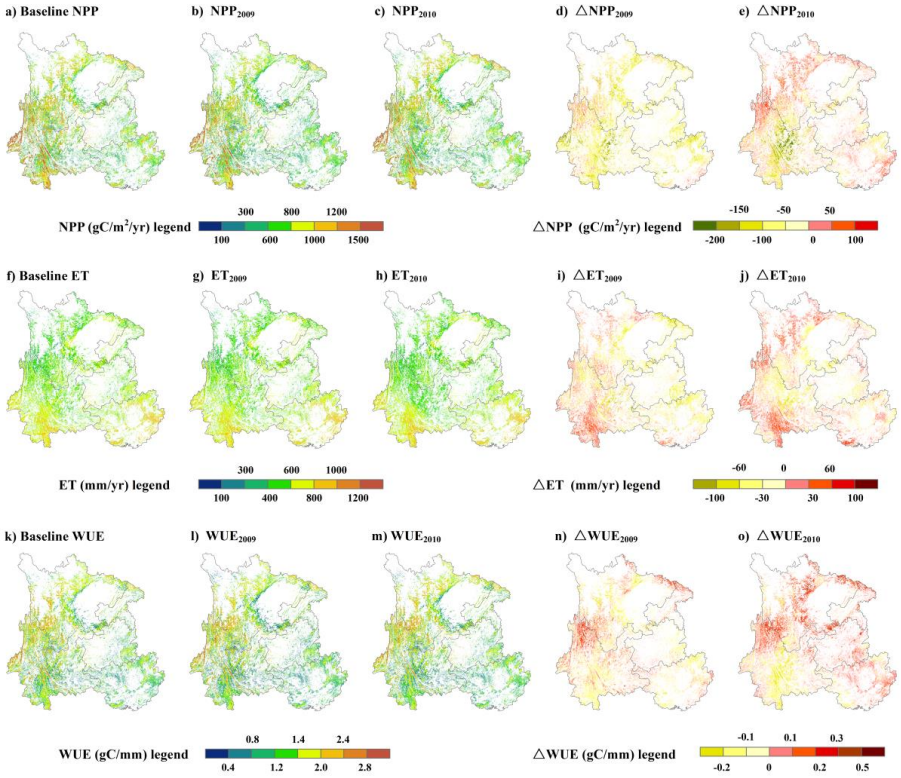

Figure 5. The spatial distribution for (**a**) baseline NPP; (**b**) NPP_{2009}; (**c**) NPP_{2010}; (**d**) $\triangle NPP_{2009}$ = NPP_{2009}-baseline NPP; (**e**) $\triangle NPP_{2010}$ = NPP_{2010}-baseline NPP; (**f**) baseline ET; (**g**) ET_{2009}; (**h**) ET_{2010}; (**i**) $\triangle ET_{2009}$ = ET_{2009}-baseline ET; (**j**) $\triangle ET_{2010}$ = ET_{2010}-baseline ET; (**k**) baseline WUE; (**l**) WUE_{2009}; (**m**) WUE_{2010}; (**n**) $\triangle WUE_{2009}$ = WUE_{2009}-baseline WUE; (**o**) $\triangle WUE_{2010}$ = WUE_{2010}-baseline WUE.

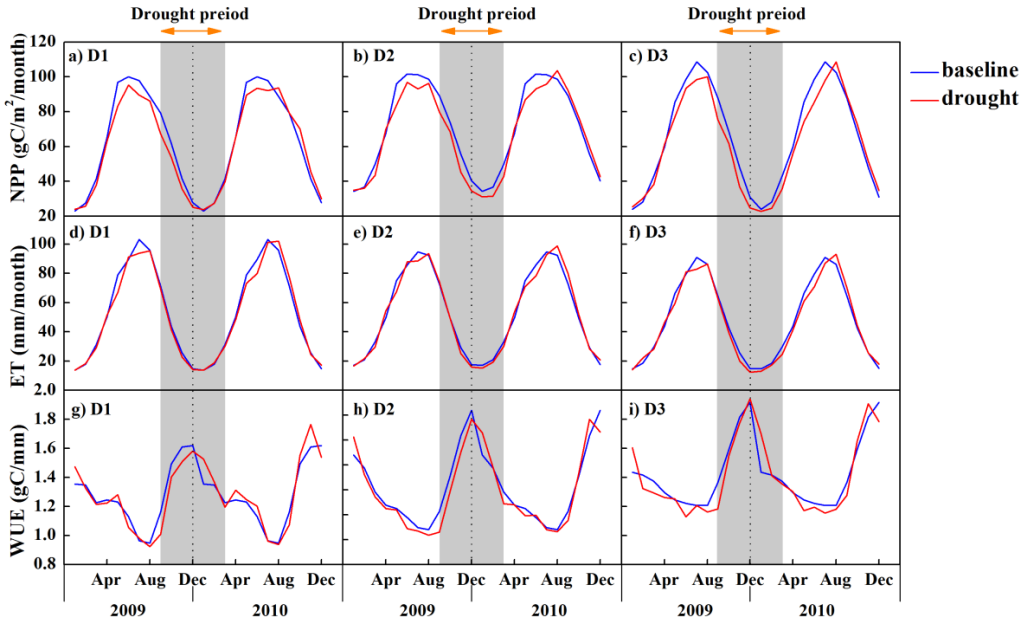

Figure 6. The time series of NPP (**a**–**c**), ET (**d**–**f**), and WUE (**g**–**i**) under the normal condition and drought condition extracted by drought class. Drought class: D1: Moderate drought; D2: Severe drought; D3: Extreme drought.

As illustrated by Figure 7, △NPP and △ET (the difference between drought and baseline NPP and ET) during the drought period in the three drought class regions were all smaller than

zero, which indicated that the drought reduced the NPP and ET of south-western China's forests. Furthermore, △NPP and △ET during the drought period in severe and extreme drought class regions are lower than that under the moderate drought class region. The decline of △NPP and △ET in the three drought class regions persisted until July, 2010. In the second half of 2010, △NPP and △ET increased to positive values, which indicated that NPP and ET under the drought condition recovered to the normal condition. Meanwhile, ΔWUE in December 2009 and January 2010 in the D3 region was larger than zero; meanwhile in the D1 and D2 regions, △WUE in January 2010 was larger than zero. We found that there existed a 4- to 6-month lag between most severe drought stage that occurred in January 2010 and maximum NPP and ET decline in 2010 (Figure 7). Moreover, the time-lag effect also existed between the drought event and ET declines (Figure 7a,b). By contrast, the extent of the maximum decline in NPP behaved more severely than that of ET in the drought area.

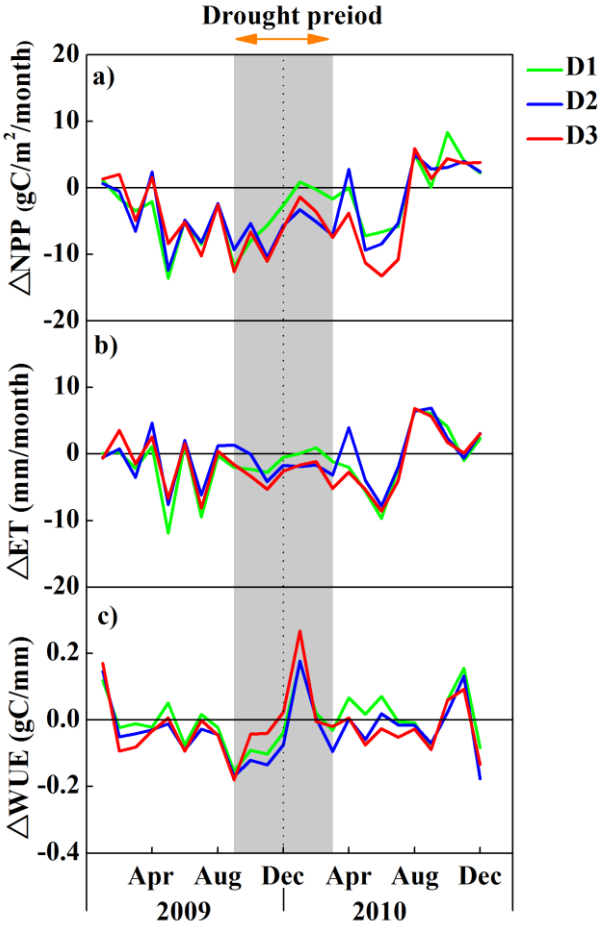

Figure 7. The time series of the difference between ecosystem measures under the drought condition (2009 and 2010) and normal condition. (**a**) △NPP = $NPP_{2009\ or\ 2010}$-baseline NPP in each drought class region; (**b**) △ET = $ET_{2009\ or\ 2010}$-baseline ET in each drought class region; (**c**) △WUE = $WUE_{2009\ or\ 2010}$-baseline WUE in each drought class region. Drought class: D1: Moderate drought; D2: Severe drought; D3: Extreme drought.

Monthly △NPP, △ET and △WUE in the extreme drought region were clarified into three vegetation types (coniferous forests, broadleaf forests, and mixed forests) (Figure 8). The changes in the △NPP and △ET for each vegetation type were similar, especially in the drought period (Sep. 2009–Mar. 2010). A similar finding about the time lag between drought and vegetation declines of NPP and ET has also been observed for all vegetation types. Furthermore, the extent of the maximum decline in NPP and ET after drought periods were similar for three vegetation types. △WUE for

each vegetation type in the extreme region was larger than zero after December, 2009 (Figure 8c). By contrast, △WUE for coniferous forests in the extreme region was larger than the other two forest types in January 2010.

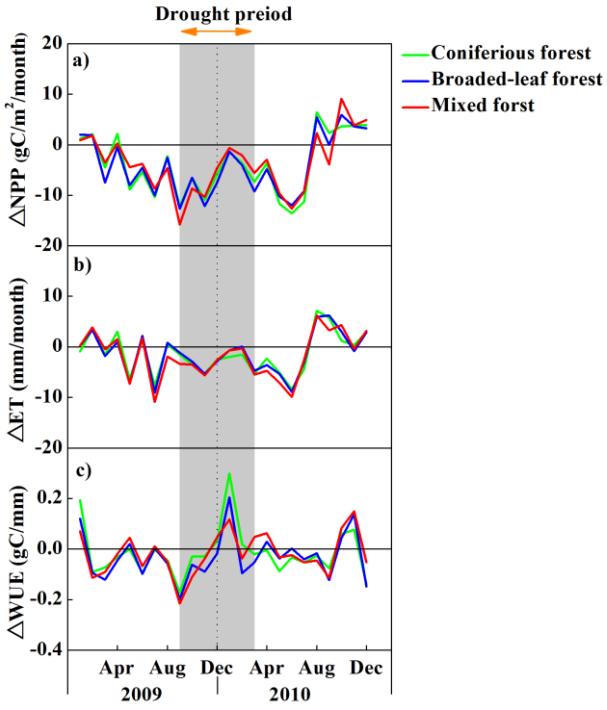

Figure 8. The time series of the difference between ecosystem measures under the drought condition (2009 and 2010) and normal condition in extreme drought (SPI < −2.0) for three vegetation types (coniferous forest, broadleaf forest, and mixed forest). (**a**) △NPP = $NPP_{2009\ or\ 2010}$-baseline NPP in D3 (extreme drought); (**b**) △ET = $ET_{2009\ or\ 2010}$-baseline ET in D3 (extreme drought); (**c**) △WUE = $WUE_{2009\ or\ 2010}$-baseline WUE in D3 (extreme drought).

4. Discussion

In our study, NPP and ET showed synchronized declines in drought periods (Figure 6). Evidence justified the idea that climate extremes such as droughts could lead to a decrease in ecosystem carbon stocks at regional and global scales [3], and had the potential to modify carbon budgets [17,60]. This can be explained by the fact that water stress decreases stomatal conductance and then affects photosynthetic biochemical processes [61]. Accompanied with the depression of productivity, canopy transpiration is usually decreased due to stomatal closure. So, reduction in precipitation alone could reduce forest ET because of the reduction in canopy interception, soil evaporation, and tree transpiration [62]. Transpiration and photosynthesis are tightly coupled via leaf stomatal conductance and environmental stress, such as water availability, temperature, and so on [63]. Furthermore, drought-induced NPP decline was more extensive than ET reduction (Figures 6 and 7). This can be explained by NPP decreasing faster than ET with an increase in aridity in the regions of lower precipitation. Some studies indicated that different sensitivity of the ecosystem process to changes in hydro-climatic conditions for sub-humid ecosystems was controlled by biological process (i.e., GPP) [32]. Moderate droughts generally do not cause large decrease in NPP due to the buffering capacity of forest soils and shallow groundwater [64]. However, extreme droughts greatly reduced the NPP of forests in this study.

In our study, the extreme drought event has the same time-lag impact on productivity and ET of the subtropical forest ecosystem in south-western China after spring 2010 (Figure 7). Furthermore, the more severe the extent of drought, the larger the time-lag impacts on NPP (Figure 7a). However,

the time-lag impacts on ET were similar between drought classes (Figure 7b). Evidence is mounting that a time-lag effect generally exists between the onset of a water shortage and the identification of its consequences [30]. For instance, hydraulic redistribution that occurred in ecosystems containing woody plants with dimorphic root systems may facilitate the nutrition acquisition and delay the onset of soil drying during the drought period [65,66]. The time-lag effect of drought on the carbon sequestration of forests can be explained by the evidence that the impact of drought on vegetation does occur instantaneously but is cumulative [67]. Meanwhile, drought persisting to next year's spring may constrain annual carbon uptake by regulating the availability of soil moisture during the summer season [68,69]. Furthermore, the time lag between drought events and greenness index as the vegetation indicators has also been reported in many studies. For example, the 3-month SPI has the best correlation with normalized difference vegetation index NDVI, indicating lag and cumulative effects of drought on vegetation [66]. Yang et al., (1997) and Wang et al., (2003) found that NDVI response to precipitation was 5–7 weeks lag for all ecosystem types in the U.S.A and 4–8 weeks in the central Great Plains, USA, respectively [70,71]. Similar findings about time-lag between drought and tree declines have also been observed in tropical [22] and in temperate regions [72].

Many studies showed that drought leads to a significant uptrend in the WUE of forests [21,33,73,74]. However, it was more complex than we have assumed in humid regions [75]. In our study, we found higher WUE occurred in extreme and severe drought regions but the changes in WUE from baseline condition to drought condition were not obvious. It seems that the forest ecosystems in subtropical China were relatively stable. In detail, WUE in the D2 and D3 regions were higher than that in D1 region in the drought period (Figure 6) or in whole year (Table 1). The results indicated that NPP was more sensitive to drought than that of ET. An increase of WUE in January 2010 was found in extreme, severe and moderate drought regions related to the baseline condition, with a value of 19%, 11% and 13%, respectively. These values were a little higher than another study in which an increase (7.09%) of WUE was observed in evergreen forests under drought stress based on global MODIS GPP and ET products [18]. An increasing trend in WUE for different drought severity (D1–D3) provided a great capacity to maintain productivity when plants were limited by water stress [33], which indicated how the forest ecosystems behaved a drought-resilient ecosystem [32,71]. Severe droughts enhance ecosystem resistance and resilience in responding to water deficiency [73], which likely contributed to the high WUE in the drought period in south-western China. Meanwhile, the synthetic declines of NPP and ET in the growing season of 2010 resulted in no obvious change of WUE in the growing season after the spring drought in 2010. We also tested the different responses of WUE to drought for each forest type (Figure 8). Similar patterns can be observed for the changes in WUE for each forest types in the extreme drought region. Furthermore, a substantial increase in WUE in the forest can also be influenced by other processes, i.e., CO_2 fertilization. But increasing atmospheric CO_2 should lead to an increase in both photosynthetic uptake and WUE [76], which was different to drought that would reduce the forests' productivity and increase the WUE.

Although forest ecosystems were sensitive to drought and temperature extremes in extreme climate events [77], our findings indicated these forests in subtropical regions were less vulnerable than commonly assumed, which can be ascribed to the rich vegetation and species diversity and high temperature and precipitation after extreme climate events in south-western China [37]. The resilience of the forest ecosystem is associated with its biological resources, species composition and ecological functions under changing climatic conditions [78]. High species diversity can partly offset the effect of extreme climate events on the carbon cycle of forests [79]. Meanwhile, it could be partly attributed to the existence of cross-scale interaction between ecological processes that will balance or offset the losses caused by extreme events. To some extent, the tree species diversity of subtropical forests in southern China alleviates the impacts imposed by extreme events, and thus the subtropical forests have higher potential to recover from disturbances.

Thus, with increasing frequencies and intensities of climate extremes in the future, studies on the response of the ecosystem carbon cycle to various levels of climate extremes are of high priority.

The gap between experiments, remote-sensing information and ecosystem modeling still exists [80]. It is necessary to monitor strategies and variables which are most useful for quantifying resilience and thresholds in wide range of ecosystems [81]. Monitoring systems with high accuracies and improvements on spatio-temporal resolution are strongly recommended to obtain better insights into the response of forest ecosystem to extreme events and feedbacks between them.

Author Contributions: L.Z. and S.W. designed the framework of this study; L.Z., W.J., K.H., Y.C., M.W. and Q.Y. collected and processed the data. L.Z., S.W., K.H. and M.W. analyzed the data and wrote the paper. W.J., R.M. and Y.C. provided suggestions on the structure of the manuscript.

Acknowledgments: This research received financial support from the National Key Research and Development Program of China from MOST (2016YFB0501501; 2017YFB0504000; 2017YFC0503803), the National Natural Science Foundation of China (41401110, 31400393) and Open Fund of State Key Laboratory of Remote Sensing Science (OFSLRSS201405) and State key laboratory of Resources and Environmental Information System. We obtained the soil data from Beijing Normal University, China (http://globalchange.bnu.edu.cn/), meteorological data from China Meteorological Administration (http://cdc.cma.gov.cn/), and ESA CCI soil moisture from the CCI SM project (http://www.esa-soilmoisture-cci.org). Special thanks go to the data provider from ChinaFLUX networks. We would like to acknowledge Yibo Liu for the assistance in producing LAI datasets. We would also like to thank Hao Shi for the assistance in scaling up the ET flux data.

Conflicts of Interest: The authors declare no conflict of interest.

References

1. Ciais, P.; Reichstein, M.; Viovy, N.; Granier, A.; Ogée, J.; Allard, V.; Aubinet, M.; Buchmann, N.; Bernhofer, C.; Carrara, A.; et al. Europe-wide reduction in primary productivity caused by the heat and drought in 2003. *Nature* **2005**, *437*, 529–533. [CrossRef] [PubMed]
2. Zeng, N.; Qian, H.F.; Roedenbeck, C.; Heimann, M. Impact of 1998–2002 midlatitude drought and warming on terrestrial ecosystem and the global carbon cycle. *Geophys. Res. Lett.* **2005**, *32*, L22709. [CrossRef]
3. Zhao, M.S.; Running, S.W. Drought-induced reduction in global terrestrial net primary production from 2000 through 2009. *Science* **2010**, *329*, 940–943. [CrossRef] [PubMed]
4. Allen, C.D.; Macalady, A.K.; Chenchouni, H.; Bachelet, D.; McDowell, N.; Vennetier, M.; Kitzberger, T.; Rigling, A.; Breshears, D.D.; (Ted) Hogg, E.H.; et al. A global overview of drought and heat-induced tree mortality reveals emerging climate change risks for forests. *For. Ecol. Manag.* **2010**, *259*, 660–684. [CrossRef]
5. Peng, C.H.; Ma, Z.H.; Lei, X.D.; Zhu, Q.; Chen, H.; Wang, W.; Liu, S.; Li, W.; Fang, X.; Zhou, X. A drought-induced pervasive increase in tree mortality across Canada's boreal forests. *Nat. Clim. Chang.* **2011**, *1*, 467–471. [CrossRef]
6. Xu, X.T.; Piao, S.L.; Wang, X.H.; Chen, A.; Ciais, P.; Myneni, R.B. Spatio-temporal patterns of the area experiencing negative vegetation growth anomalies in China over the last three decades. *Environ. Res. Lett.* **2012**, *7*, 035701. [CrossRef]
7. Huang, C.Y.; Anderegg, W.R.L. Large drought-induced aboveground live biomass losses in southern Rocky Mountain aspen forests. *Glob. Chang. Biol.* **2012**, *18*, 1016–1027. [CrossRef]
8. Anderegg, L.D.L.; Anderegg, W.R.L.; Abatzoglou, J.; Hausladen, A.M.; Berry, J.A. Drought characteristics' role in widespread aspen forest mortality across Colorado, USA. *Glob. Chang. Biol.* **2013**, *19*, 1526–1537. [CrossRef] [PubMed]
9. Easterling, D.R.; Meehl, G.A.; Parmesan, C.; Changnon, S.A.; Karl, T.R.; Mearns, L.O. Climate extremes: Observations, modeling, and impacts. *Science* **2000**, *289*, 2068–2074. [CrossRef] [PubMed]
10. Schwalm, C.R.; Williams, C.A.; Schaefer, K.; Baldocchi, B.D.; Black, T.A.; Goldstein, A.H.; Law, B.E.; Oechel, W.C.; Paw U, K.T.; Scott, R.L. Reduction in carbon uptake during turn of the century drought in western North America. *Nat. Geosci.* **2012**, *5*, 551–556. [CrossRef]
11. Trenberth, K.E.; Dai, A.; Van Der Schrier, G.; Jones, P.D.; Barichivich, J.; Briffa, K.R.; Sheffield, J. Global warming and changes in drought. *Nat. Clim. Chang.* **2014**, *4*, 17–22. [CrossRef]
12. Meehl, G.A.; Tebaldi, C. More intense, more frequent, and longer lasting heat waves in the 21st century. *Science* **2004**, *305*, 994–997. [CrossRef] [PubMed]
13. Gu, L.; Hanson, P.J.; Post, W.M.; Kaiser, D.P.; Yang, B.; Nemani, R.; Pallardy, S.G.; Meyers, T. The 2007 eastern US spring freezes: Increased cold damage in a warming world? *Bioscience* **2008**, *58*, 253–262. [CrossRef]

14. Stone, R. Natural disasters—Ecologists report huge storm losses in China's forests. *Science* **2008**, *319*, 1318–1319. [CrossRef] [PubMed]
15. Saatchi, S.; Asefi-Najafabady, S.; Malhi, Y.; Aragão, L.E.O.C.; Anderson, L.O.; Myneni, R.B.; Nemani, R. Persistent effects of a severe drought on Amazonian forest canopy. *Proc. Natl. Acad. Sci. USA* **2013**, *110*, 565–570. [CrossRef] [PubMed]
16. Frolking, S.; Palace, M.W.; Clark, D.B.; Chambers, J.Q.; Shugart, H.H.; Hurtt, G.C. Forest disturbance and recovery: A general review in the context of spaceborne remote sensing of impacts on aboveground biomass and canopy structure. *J. Geophys. Res. Biogeosci.* **2009**, *114*, G00E02. [CrossRef]
17. Frank, D.; Reichstein, M.; Bahn, M.; Thonicke, K.; Frank, D.; Mahecha, M.D.; Smith, P.; van der Velde, M.; Vicca, S.; Babst, F.; et al. Effects of climate extremes on the terrestrial carbon cycle: Concepts, processes and potential future impacts. *Glob. Chang. Biol.* **2015**, *21*, 2861–2880. [CrossRef] [PubMed]
18. Yu, Z.; Wang, J.; Liu, S.; Rentch, J.S.; Sun, P.; Lu, C. Global gross primary productivity and water use efficiency changes under drought stress. *Environ. Res. Lett.* **2017**, *12*, 014016. [CrossRef]
19. Nemani, R.R.; Keeling, C.D.; Hashimoto, H.; William, M.J.; Stephen, C.P.; Compton, J.T.; Ranga, B.M.; Steven, W.R. Climate-driven increases in global terrestrial net primary production from 1982 to 1999. *Science* **2003**, *300*, 1560–1563. [CrossRef] [PubMed]
20. Reichstein, M.; Bahn, M.; Ciais, P.; Frank, D.; Mahecha, M.D.; Seneviratne, S.I.; Zscheischler, J.; Beer, C.; Buchmann, N.; Frank, D.C.; et al. Climate extremes and the carbon cycle. *Nature* **2013**, *500*, 287–295. [CrossRef] [PubMed]
21. Anderegg, W.R.L.; Berry, J.A.; Smith, D.D.; Sperry, J.; Anderegg, L.; Field, C.B. The roles of hydraulic and carbon stress in a widespread climate-induced forest die-off. *Proc. Natl. Acad. Sci. USA* **2012**, *109*, 233–237. [CrossRef] [PubMed]
22. Reichstein, M.; Ciais, P.; Papale, D.; Valentini, R.; Running, S.W.; Viovy, N.; Cramer, W.; Granier, A.; Ogée, J.; Allard, V.; et al. Reduction of ecosystem productivity and respiration during the European summer 2003 climate anomaly: A joint flux tower, remote sensing and modelling analysis. *Glob. Chang. Biol.* **2007**, *13*, 634–651. [CrossRef]
23. Phillips, O.L.; van der Heijden, G.; Lewis, S.L.; López-González, G.; Aragão, L.E.; Lloyd, J.; Malhi, Y.; Monteagudo, A.; Almeida, S.; Dávila, E.A.; et al. Drought-mortality relationships for tropical forests. *New Phytol.* **2010**, *187*, 631–646. [CrossRef] [PubMed]
24. Potter, C.; Klooster, S.; Hiatt, C.; Genovese, V.; Castilla-Rubio, J.C. Changes in the carbon cycle of Amazon ecosystems during the 2010 drought. *Environ. Res. Lett.* **2011**, *6*. [CrossRef]
25. Mu, Q.; Heinsch, F.A.; Zhao, M.; Running, S.W. Development of a global evapotranspiration algorithm based on MODIS and global meteorology data. *Remote Sens. Environ.* **2007**, *111*, 519–536. [CrossRef]
26. Alton, P.; Fisher, R.; Los, S.; Williams, M. Simulations of global evapotranspiration using semiempirical and mechanistic schemes of plant hydrology. *Glob. Biogeochem. Cycles* **2009**, *23*, GB4023. [CrossRef]
27. Jung, M.; Reichstein, M.; Ciais, P.; Seneviratne, S.I.; Sheffield, J.; Goulden, M.L.; Bonan, G.; Cescatti, A.; Chen, J.; de Jeu, R.; et al. Recent decline in the global land evapotranspiration trend due to limited moisture supply. *Nature* **2010**, *467*, 951–954. [CrossRef] [PubMed]
28. Wang, K.; Dickinson, R.E. A review of global terrestrial evapotranspiration: Observation, modeling, climatology, and climatic variability. *Rev. Geophys.* **2012**, *50*. [CrossRef]
29. Breshears, D.D.; Cobb, N.S.; Rich, P.M.; Price, K.P.; Allen, C.D.; Balice, R.G.; Romme, W.H.; Kastens, J.H.; Floyd, M.L.; Belnap, J.; et al. Regional vegetation die-off in response to global-change-type drought. *Proc. Natl. Acad. Sci. USA* **2005**, *102*, 15144–15148. [CrossRef] [PubMed]
30. Vicente-Serrano, S.M.; Gouveia, C.; Camarero, J.J.; Beguería, S.; Trigo, R.; López-Moreno, J.I.; Azorín-Molina, C.; Pasho, E.; Lorenzo-Lacruz, J.; Revuelto, J.; et al. Response of vegetation to drought time-scales across global land biomes. *Proc. Natl. Acad. Sci. USA* **2013**, *110*, 52–57. [CrossRef] [PubMed]
31. Tang, X.; Li, H.; Desai, A.R.; Nagy, Z.; Luo, J.; Kolb, T.E.; Olioso, A.; Xu, X.; Yao, L.; Kutsch, W.; et al. How is water-use efficiency of terrestrial ecosystems distributed and changing on Earth? *Sci. Rep.* **2014**, *4*, 7483. [CrossRef] [PubMed]
32. Yang, Y.; Guan, H.; Batelaan, O.; McVicar, T.R.; Long, D.; Piao, S.; Liang, W.; Liu, B.; Jin, Z.; Simmons, C.T. Contrasting responses of water use efficiency to drought across global terrestrial ecosystems. *Sci. Rep.* **2016**, *6*, 23284. [CrossRef] [PubMed]

33. Ponce-Campos, G.E.; Moran, M.S.; Huete, A.; Zhang, Y.; Bresloff, C.; Huxman, T.E.; Eamus, D.; Bosch, D.D.; Buda, A.R.; Gunter, S.A.; et al. Ecosystem resilience despite large-scale altered hydroclimatic conditions. *Nature* **2013**, *494*, 349–352. [CrossRef] [PubMed]
34. Tian, H.; Chen, G.; Liu, M.; Zhang, C.; Sun, G.; Lu, C.; Xu, X.; Ren, W.; Pan, S.; Chappelka, A. Model estimates of net primary productivity, evapotranspiration, and water use efficiency in the terrestrial ecosystems of the southern United States during 1895–2007. *For. Ecol. Manag.* **2010**, *259*, 1311–1327. [CrossRef]
35. Wu, Z.Y.; Lu, G.H.; Wen, L.; Lin, C.A. Reconstructing and analyzing China's fifty-nine year (1951–2009) drought history using hydrological model simulation. *Hydrol. Earth Syst. Sci.* **2011**, *15*, 2881–2894. [CrossRef]
36. Yang, J.; Gong, D.Y.; Wang, W.S.; Hu, M.; Mao, R. Extreme drought event of 2009/2010 over southwestern China. *Meteorol. Atmos. Phys.* **2012**, *115*, 173–184. [CrossRef]
37. Zhang, L.; Xiao, J.; Li, J.; Wang, K. The 2010 spring drought reduced primary productivity in southwestern China. *Environ. Res. Lett.* **2012**, *7*, 045706. [CrossRef]
38. Dai, L.M.; Wang, Y.; Su, D.K.; Zhou, L.; Yu, D.P.; Lewis, B.J.; Qi, L. Major forest types and the evolution of sustainable forestry in china. *Environ. Manag.* **2011**, *48*, 1066–1078. [CrossRef] [PubMed]
39. McKee, T.B.; Doesken, N.J.; Kleist, J. The relationship of drought frequency and duration to time scales. In Proceedings of the 8th Conference on Applied Climatology, Anaheim, CA, USA, 17–22 January 1993; pp. 179–184.
40. Liu, J.; Chen, J.M.; Cihlar, J.; Park, W.M. A process-based boreal ecosystem productivity simulator using remote sensing inputs. *Remote Sens. Environ.* **1997**, *62*, 158–175. [CrossRef]
41. Chen, J.M.; Liu, J.; Cihlar, J.; Goulden, M.L. Daily canopy photosynthesis model through temporal and spatial scaling for remote sensing applications. *Ecol. Model.* **1999**, *124*, 99–119. [CrossRef]
42. Niu, S.; Xing, X.; Zhang, Z.; Xia, J.Y.; Zhou, X.H.; Song, B.; Li, L.H.; Wan, S.Q. Water-use efficiency in response to climate change: From leaf to ecosystem in a temperate steppe. *Glob. Chang. Biol.* **2011**, *17*, 1073–1082. [CrossRef]
43. Liu, Y.B.; Xiao, J.F.; Ju, W.M.; Zhou, Y.L.; Wang, S.Q.; Wu, X.C. Water use efficiency of China's terrestrial ecosystems and responses to drought. *Sci. Rep.* **2015**, *5*, 13799. [CrossRef] [PubMed]
44. Running, S.W.; Coughlan, J.C. A General-Model of Forest Ecosystem Processes for Regional Applications. I. Hydrologic Balance, Canopy Gas-Exchange and Primary Production Processes. *Ecol. Model.* **1988**, *42*, 125–154. [CrossRef]
45. Farquhar, G.D.; von Caemmerer, S.; Berry, J.A. A biochemical model of photosynthetic CO_2 assimilation in leaves of C3 species. *Planta* **1980**, *149*, 78–90. [CrossRef] [PubMed]
46. Monteith, J.L. Evaporation and Environment. *Symp. Soc. Exp. Biol.* **1965**, *19*, 205–234. [PubMed]
47. Feng, X.; Liu, G.H.; Chen, J.M.; Chen, M.; Liu, J.; Ju, W.M.; Sun, R.; Zhou, W. Net primary productivity of China's terrestrial ecosystems from a process model driven by remote sensing. *J. Environ. Manag.* **2007**, *85*, 563–573. [CrossRef] [PubMed]
48. Ju, W.; Wang, S.; Yu, G.; Zhou, Y.; Wang, H. Modeling the impact of drought on canopy carbon and water fluxes for a subtropical evergreen coniferous plantation in southern China through parameter optimization using an ensemble Kalman filter. *Biogeosciences* **2010**, *7*, 845–857. [CrossRef]
49. Liu, Y.B.; Ju, W.M.; He, H.L.; Wang, S.Q.; Sun, R.; Zhang, Y.D. Changes of net primary productivity in China during recent 11 years detected using an ecological model driven by MODIS data. *Front. Earth Sci.* **2013**, *7*, 112–127. [CrossRef]
50. Ju, W.M.; Chen, J.M.; Black, T.A.; Barr, A.G.; Liu, J.; Chen, B.Z. Modelling multi-year coupled carbon and water fluxes in a boreal aspen forest. *Agric. For. Meteorol.* **2006**, *140*, 136–151. [CrossRef]
51. Zhang, F.M.; Chen, J.M.; Chen, J.Q.; Gough, C.M.; Martin, T.A.; Dragoni, D. Evaluating spatial and temporal patterns of MODIS GPP over the conterminous US against flux measurements and a process model. *Remote Sens. Environ.* **2012**, *124*, 717–729. [CrossRef]
52. Zhang, F.M.; Ju, W.M.; Shen, S.H.; Wang, S.Q.; Yu, G.R. Variations of Terrestrial Net Primary Productivity in East Asia. *Terr. Atmos. Ocean Sci.* **2012**, *23*, 425–437. [CrossRef]
53. Chen, J.M.; Mo, G.; Pisek, J.; Liu, J.; Deng, F.; Ishizawa, M.; Chan, D. Effects of foliage clumping on the estimation of global terrestrial gross primary productivity. *Glob. Biogeochem. Cycles* **2012**, *26*, GB1019. [CrossRef]
54. Zhu, X.D.; He, H.L.; Liu, M.; Yu, G.R.; Sun, X.M.; Gao, Y.H. Spatio-temporal variation of photosynthetically active radiation in China in recent 50 years. *J. Geogr. Sci.* **2010**, *20*, 803–817. [CrossRef]

55. Deng, F.; Chen, J.M.; Plummer, S.; Chen, M.; Pisek, J. Algorithm for global leaf area index retrieval using satellite imagery. *IEEE Trans. Geosci. Remote Sens.* **2006**, *44*, 2219–2229. [CrossRef]
56. Chen, J.M.; Deng, F.; Chen, M.Z. Locally adjusted cubic-spline capping for reconstructing seasonal trajectories of a satellite-derived surface parameter. *IEEE Trans. Geosci. Remote Sens.* **2006**, *44*, 2230–2238. [CrossRef]
57. Shangguan, W.; Dai, Y.J.; Liu, B.Y.; Ye, A.; Yuan, H. A soil particle-size distribution dataset for regional land and climate modelling in China. *Geoderma* **2012**, *171*, 85–91. [CrossRef]
58. Yu, G.R.; Song, X.; Wang, Q.F.; Liu, Y.F.; Guan, D.X.; Yan, J.H.; Sun, X.M.; Zhang, L.M.; Wen, X.F. Water-use efficiency of forest ecosystems in eastern China and its relations to climatic variables. *New Phytol.* **2008**, *177*, 927–937. [CrossRef] [PubMed]
59. Zhu, X.J.; Yu, G.R.; Wang, Q.F.; Hu, Z.M.; Zheng, H.; Li, S.G.; Sun, X.M.; Zhang, Y.P.; Yan, J.H.; Wang, H.M.; et al. Spatial variability of water use efficiency in China's terrestrial ecosystems. *Glob. Planet. Chang.* **2015**, *129*, 37–44. [CrossRef]
60. Zeng, H.C.; Chambers, J.Q.; Negrón-Juarez, R.I.; George, C.H.; David, B.B.; Mark, D. Powellc.Impacts of tropical cyclones on US forest tree mortality and carbon flux from 1851 to 2000. *Proc. Natl. Acad. Sci. USA* **2009**, *106*, 7888–7892. [CrossRef] [PubMed]
61. Zhou, L.; Wang, S.; Chi, Y.; Zhou, L.; Wang, S.; Chi, Y.; Li, Q.; Huang, K.; Yu, Q. Responses of photosynthetic parameters to drought in subtropical forest ecosystem of China. *Sci. Rep.* **2015**, *5*, 18254. [CrossRef] [PubMed]
62. Sun, S.L.; Ge, S.; Peter, C.; Steven, G.M.; Erika, C.; Xiao, J.F.; Zhang, Y. Drought impacts on ecosystem functions of the U.S. National Forests and Grasslands: Part I evaluation of a water and carbon balance model. *For. Ecol. Manag.* **2015**, *353*, 260–268. [CrossRef]
63. Sun, Y.; Piao, S.; Huang, M.; Sun, Y.; Piao, S.L.; Huang, M.T.; Ciais, P.; Zeng, Z.Z.; Cheng, L.; Li, X.R.; et al. Global patterns and climate drivers of water-use efficiency in terrestrial ecosystems deduced from satellite-based datasets and carbon cycle models. *Glob. Ecol. Biogeogr.* **2016**, *25*, 311–323. [CrossRef]
64. Teuling, A.; Seneviratne, S.I.; Stöckli, R.; Reichstein, M.; Moors, E.; Ciais, P.; Luyssaert, S.; van den Hurk, B.; Ammann, C.; Bernhofer, C.; et al. Contrasting response of European forest and grassland energy exchange to heatwaves. *Nat. Geosci.* **2010**, *3*, 722–727. [CrossRef]
65. Bleby, T.M.; McElrone, A.J.; Jackson, R.B. Water uptake and hydraulic redistribution across large woody root systems to 20 m depth. *Plant Cell Environ.* **2010**, *33*, 2132–2148. [CrossRef] [PubMed]
66. Neumann, R.B.; Cardon, Z.G. The magnitude of hydraulic redistribution by plant roots: A review and synthesis of empirical and modeling studies. *New Phytol.* **2012**, *194*, 337–352. [CrossRef] [PubMed]
67. Ji, L.; Peters, A.J. Assessing vegetation response to drought in the northern Great Plains using vegetation and drought indices. *Remote Sens. Environ.* **2003**, *87*, 85–98. [CrossRef]
68. Kwon, H.; Pendall, E.; Ewers, B.E.; Cleary, M.; Naithani, K. Spring drought regulates summer net ecosystem CO_2 exchange in a sagebrush-steppe ecosystem. *Agric. For. Meteorol.* **2008**, *148*, 381–391. [CrossRef]
69. Scott, R.L.; Jenerette, G.D.; Potts, D.L.; Huxman, T.E. Effects of seasonal drought on net carbon dioxide exchange from a woody-plant-encroached semiarid grassland. *J. Geophys. Res. Biogeosci.* **2009**, *114*, G04004. [CrossRef]
70. Yang, W.; Yang, L.; Merchant, J.W. An assessment of AVHRR/NDVI ecoclimatological relations in Nebraska, USA. *Int. J. Remote Sens.* **1997**, *18*, 2161–2180. [CrossRef]
71. Wang, J.; Rich, P.M.; Price, K.P. Temporal responses of NDVI to precipitation and temperature in the central Great Plains, USA. *Int. J. Remote Sens.* **2003**, *24*, 2345–2364. [CrossRef]
72. Bréda, N.; Huc, R.; Granier, A.; Dreyer, E. Temperate forest trees and stands under severe drought: A review of ecophysiological responses, adaptation processes and long-term consequences. *Ann. For. Sci.* **2006**, *63*, 625–644. [CrossRef]
73. Malone, S.L.; Tulbure, M.G.; Pérez-Luque, A.J.; Assal, T.J.; Bremer, L.L.; Drucker, D.P.; Hillis, V.; Varela, S.; Goulden, M. Drought resistance across California ecosystems: Evaluating changes in carbon dynamics using satellite imagery. *Ecosphere* **2016**, *7*. [CrossRef]
74. Krishnan, P.; Black, T.A.; Grant, N.J.; Barr, A.G.; Hogg, E.H.; Jassal, R.S.; Morgenstern, K. Impact of changing soil moisture distribution on net ecosystem productivity of a boreal aspen forest during and following drought. *Agric. For. Meteorol.* **2006**, *139*, 208–223. [CrossRef]
75. Huang, L.; He, B.; Han, L.; Liu, J.; Wang, H.; Chen, Z. A global examination of the response of ecosystem water-use efficiency to drought based on MODIS data. *Sci. Total Environ.* **2017**, *601–602*, 1097–1107. [CrossRef] [PubMed]

76. Keenan, T.F.; Hollinger, D.Y.; Bohrer, G.; Dragoni, D.; Munger, J.W.; Schmid, H.P.; Richardson, A.D. Increase in forest water-use efficiency as atmospheric carbon dioxide concentrations rise. *Nature* **2013**, *499*, 324–327. [CrossRef] [PubMed]
77. Zelazowski, P.; Malhi, Y.; Huntingford, C.; Sitch, S.; Fisher, J.B. Changes in the potential distribution of humid tropical forests on a warmer planet. *Philos. Trans. R. Soc. A* **2011**, *369*, 137–160. [CrossRef] [PubMed]
78. Zhou, G.Y.; Peng, C.H.; Li, Y.L.; Liu, S.Z.; Zhang, Q.M.; Tang, X.L.; Liu, J.X.; Yan, J.H.; Zhang, D.Q.; Chu, G.W. A climate change-induced threat to the ecological resilience of a subtropical monsoon evergreen broad-leaved forest in Southern China. *Glob. Chang. Biol.* **2013**, *19*, 1197–1210. [CrossRef] [PubMed]
79. Tan, Z.H.; Zhang, Y.P.; Liang, N.S.; Hsia, Y.J.; Zhang, Y.J.; Zhou, G.Y.; Li, Y.L.; Juang, J.Y.; Chu, H.S.; Yan, J.H.; et al. An observational study of the carbon-sink strength of East Asian subtropical evergreen forests. *Environ. Res. Lett.* **2012**, *7*. [CrossRef]
80. Liu, S.G.; Bond-Lamberty, B.; Hicke, J.; Vargas, R.; Zhao, S.Q.; Chen, J.; Edburg, S.L.; Hu, Y.M.; Liu, J.X.; McGuire, A.D.; et al. Simulating the impacts of disturbances on forest carbon cycling in North America: Processes, data, models, and challenges. *J. Geophys. Res. Biogeosci.* **2011**, *116*, G00K08. [CrossRef]
81. Batt, R.D.; Carpenter, S.R.; Cole, J.J.; Pace, M.L.; Johnson, R.A. Changes in ecosystem resilience detected in automated measures of ecosystem metabolism during a whole-lake manipulation. *Proc. Natl. Acad. Sci. USA* **2013**, *110*, 17398–17403. [CrossRef] [PubMed]